Single parameter optimization for simultaneous automatic compensation of multiple orders of dispersion for a 1.28 Tbaud signal

Yvan Paquot,[1,*] Jochen Schröder,[1] Jürgen Van Erps,[1,2] Trung D. Vo,[1] Mark D. Pelusi,[1] Steve Madden,[3] Barry Luther-Davies,[3] and Benjamin J. Eggleton[1]

[1,*]*Centre for Ultrahigh bandwidth Devices for Optical Systems (CUDOS), Institute of Photonics and Optical Science (IPOS) School of Physics A28, University of Sydney, NSW 2006, Australia*
[2]*Vrije Universiteit Brussel, Brussels Photonics Team, Dept. of Applied Physics and Photonics, Pleinlaan 2, 1050 Brussel, Belgium*
[3]*CUDOS, Laser Physics Centre, Australian National Univ., Canberra A.C.T. 0200, Australia*
[*]*yvan@physics.usyd.edu.au*

Abstract: We report the demonstration of automatic higher-order dispersion compensation for the transmission of 275 fs pulses associated with a Tbaud Optical Time Division Multiplexed (OTDM) signal. Our approach achieves simultaneous automatic compensation for 2^{nd}, 3^{rd} and 4^{th} order dispersion using an LCOS spectral pulse shaper (SPS) as a tunable dispersion compensator and a dispersion monitor made of a photonic-chip-based all-optical RF-spectrum analyzer. The monitoring approach uses a single parameter measurement extracted from the RF-spectrum to drive a multidimensional optimization algorithm. Because these pulses are highly sensitive to fluctuations in the GVD and higher orders of chromatic dispersion, this work represents a key result towards practical transmission of ultrashort optical pulses. The dispersion can be adapted on-the-fly for a 1.28 Tbaud signal at any place in the transmission line using a black box approach.

OCIS codes: (060.2330) Fiber optics communications; (060.4256) Networks, network optimization.

References and links

1. I. P. Kaminow, T. Li, and A. E. Willner, *Optical Fiber Telecommunications V A: Components and Subsystems*, Volume 1 (Academic Press, 2008).
2. A. Gnauck, G. Charlet, P. Tran, P. Winzer, C. Doerr, J. Centanni, E. Burrows, T. Kawanishi, T. Sakamoto, and K. Higuma, "25.6-Tb/s WDM Transmission of Polarization-Multiplexed RZ-DQPSK Signals," J. Lightwave Technol. **26**, 79–84 (2008).
3. D. Qian, M.-F. Huang, E. Ip, Y.-K. Huang, Y. Shao, J. Hu, and T. Wang, "101.7-Tb/s (370294-Gb/s) PDM-128QAM-OFDM Transmission over 355-km SSMF using Pilot-based Phase Noise Mitigation - OSA Technical Digest (CD)," in "Optical Fiber Communication Conference," (Optical Society of America, 2011), p. PDPB5.
4. P. Winzer and R. Essiambre, "Advanced Optical Modulation Formats," Proceedings of the IEEE **94**, 952–985 (2006).

#155613 - $15.00 USD Received 30 Sep 2011; revised 15 Nov 2011; accepted 19 Nov 2011; published 30 Nov 2011

5. H. Hansen Mulvad, L. Oxenløwe, M. Galili, A. Clausen, L. Gruner-Nielsen, and P. Jeppesen, "1.28 Tbit/s single-polarisation serial OOK optical data generation and demultiplexing," Electron. Lett. **45**, 280–281 (2009).
6. T. Richter, E. Palushani, C. Schmidt-Langhorst, M. Nölle, R. Ludwig, and C. Schubert, "Single Wavelength Channel 10.2 Tb/s TDM-Data Capacity using 16-QAM and coherent detection - OSA Technical Digest (CD)," in "Optical Fiber Communication Conference," (Optical Society of America, 2011), p. PDPA9.
7. T. D. Vo, M. D. Pelusi, J. Schröder, F. Luan, S. J. Madden, D.-Y. Choi, D. A. P. Bulla, B. Luther-Davies, and B. J. Eggleton, "Simultaneous multi-impairment monitoring of 640 Gb/s signals using photonic chip based RF spectrum analyzer." Opt. Express **18**, 3938–45 (2010).
8. G. P. Agrawal, *Nonlinear fiber optics* (Academic Press, 2001).
9. C. Poole, J. Wiesenfeld, D. Digiovanni, and A. Vengsarkar, "Optical fiber-based dispersion compensation using higher order modes near cutoff," J. Lightwave Technol. **12**, 1746–1758 (1994).
10. M. Nakazawa, T. Yamamoto, and K. R. Tamura, "1.28Tbit/s 70 km OTDM transmission using third- and fourth-order simultaneous dispersion compensation with a phase modulator," Electron. Lett. **36**, 2027–2029 (2000).
11. B. Eggleton, B. Mikkelsen, G. Raybon, A. Ahuja, J. Rogers, P. Westbrook, T. Nielsen, S. Stulz, and K. Dreyer, "Tunable dispersion compensation in a 160-Gb/s TDM system by a voltage controlled chirped fiber Bragg grating," IEEE Photon. Technol. Lett. **12**, 1022–1024 (2000).
12. M. Durkin, M. Ibsen, M. Cole, and R. Laming, "1 m long continuously-written fibre Bragg gratings for combined second-and third-order dispersion compensation," Electron. Lett. **33**, 1891–1893 (1997).
13. S. Wielandy, P. Westbrook, M. Fishteyn, P. Reyes, W. Schairer, H. Rohde, and G. Lehmann, "Demonstration of automatic dispersion control for 160 Gbit/s transmission over 275 km of deployed fibre," Electron. Lett. **40**, 690 (2004).
14. D. T. Neilson, R. Ryf, F. Pardo, V. A. Aksyuk, M.-E. Simon, D. O. Lopez, D. M. Marom, and S. Chandrasekhar, "MEMS-Based Channelized Dispersion Compensator With Flat Passbands," J. Lightwave Technol. **22**, 101– (2004).
15. G.-H. Lee, S. Xiao, and A. Weiner, "Optical Dispersion Compensator With 4000-ps/nm Tuning Range Using a Virtually Imaged Phased Array (VIPA) and Spatial Light Modulator (SLM)," IEEE Photon. Technol. Lett. **18**, 1819–1821 (2006).
16. T. Kurosu, K. Tanizawa, S. Petit, and S. Namiki, "Parametric tunable dispersion compensation for the transmission of sub-picosecond pulses," Opt. Express **19**, 15549–15559 (2011).
17. T. Kato, Y. Koyano, and M. Nishimura, "Temperature dependence of chromatic dispersion in various types of optical fiber," Opt. Lett. **25**, 1156 (2000).
18. M. Hamp, J. Wright, M. Hubbard, and B. Brimacombe, "Investigation into the temperature dependence of chromatic dispersion in optical fiber," IEEE Photon. Technol. Lett. **14**, 1524–1526 (2002).
19. M. A. F. Roelens, S. Frisken, J. A. Bolger, D. Abakoumov, G. Baxter, S. Poole, and B. J. Eggleton, "Dispersion Trimming in a Reconfigurable Wavelength Selective Switch," J. Lightwave Technol. **26**, 73–78 (2008).
20. M. Pelusi, F. Luan, T. D. Vo, M. R. E. Lamont, S. J. Madden, D. A. Bulla, D.-Y. Choi, B. Luther-Davies, and B. J. Eggleton, "Photonic-chip-based radio-frequency spectrum analyser with terahertz bandwidth," Nat. Photon. **3**, 139–143 (2009).
21. I. Shake, W. Takara, S. Kawanishi, and Y. Yamabayashi, "Optical signal quality monitoring method based on optical sampling," Electron. Lett. **34**, 2152–2154 (1998).
22. J. Van Erps, F. Luan, M. Pelusi, T. Iredale, S. Madden, D. Choi, D. Bulla, B. Luther-Davies, H. Thienpont, and B. Eggleton, "High-Resolution Optical Sampling of 640-Gb/s Data Using Four-Wave Mixing in Dispersion-Engineered Highly Nonlinear As2S3 Planar Waveguides," J. Lightwave Technol. **28**, 209–215 (2010).
23. J. Curtis and J. Carroll, "Autocorrelation systems for the measurement of picosecond pulses from injection lasers," Intern. J. Electron. **60**, 87–111 (1986).
24. P. Westbrook, S. Hunsche, G. Raybon, T. Her, and B. Eggleton, "Measurement of pulse degradation using all-optical 2R regenerator," Electron. Lett. **38**, 1193 (2002).
25. P. Westbrook, B. Eggleton, G. Raybon, and S. Hunsche, "Measurement of residual chromatic dispersion of a 40-Gb/s RZ signal via spectral broadening," IEEE Photon. Technol. Lett. **14**, 346–348 (2002).
26. C. Dorrer and D. Maywar, "RF Spectrum Analysis of Optical Signals Using Nonlinear Optics," J. Lightwave Technol. **22**, 266–274 (2004).
27. A. M. Weiner, J. P. Heritage, and E. M. Kirschner, "High-resolution femtosecond pulse shaping," J. Opt. Soc. Am. B **5**, 1563 (1988).
28. J. Van Erps, J. Schroeder, T. Vo, M. Pelusi, S. Madden, D. Choi, D. Bulla, B. Luther-Davies, and B. Eggleton, "Automatic dispersion compensation for 1 . 28Tb/s OTDM signal transmission using photonic-chip-based dispersion monitoring," Opt. Express **18**, 25415–25421 (2010).
29. T. Inoue and S. Namiki, "Pulse compression techniques using highly nonlinear fibers," Laser Photon. Rev. **2**, 83–99 (2008).
30. D.-Y. Choi, S. Madden, D. A. Bulla, R. Wang, A. Rode, and B. Luther-Davies, "Submicrometer-Thick Low-Loss As2S3 Planar Waveguides for Nonlinear Optical Devices," IEEE Photon. Technol. Lett. **22**, 495–497 (2010).

#155613 - $15.00 USD Received 30 Sep 2011; revised 15 Nov 2011; accepted 19 Nov 2011; published 30 Nov 2011

1. Introduction

The demand for bandwidth in telecommunications has been relentlessly increasing over the last decade. Various strategies have been developed to keep up with this increasing demand [1]. Common techniques are Wavelength Division Multiplexing (WDM) [2], Optical Frequency Division Multiplexing (OFDM) [3] and Advanced Modulation Formats (DQPSK, QAM, M-ASK) [4] or a combination of the above. Ultra-high symbol rate signals created by Optical Time Division Multiplexing (OTDM) of low bit-rate signals is another promising approach. Symbol-rates above 1 Tbaud have been demonstrated [5, 6] and techniques have been developed to monitor the signal quality [7]. However, these high bandwidth signals are increasingly susceptible to impairments. In addition to group velocity dispersion (GVD), higher-orders of dispersion significantly affect the transmission [8]. An accurate dispersion compensation solution is therefore crucial.

In present optical communications networks, the group velocity dispersion (GVD) of the fiber is balanced by spans of Dispersion Compensating Fiber (DCF). At Tbaud rates, this method is no longer sufficient as higher orders of dispersion must be taken into account and even slight drifts of the dispersion coefficients (for example due to temperature fluctuations) can be detrimental. Also the dispersion compensation must be extremely accurate as Tbaud pulses are broadened by a factor of 2 over a length of only 1m of standard SMF by GVD. All previous experiments employed elaborate compensation schemes using concatenated specialty fibers [9], phase modulators [10], tunable fiber Bragg gratings [11–13], MEMS [14], a spatial light modulator with a virtually imaged phase array [15] or parametric wavelength conversion [16] to compensate higher orders of dispersion. However, these compensation schemes were either static, narrow band, limited to GVD or did not include a dispersion measurement system. Therefore they were unable to compensate for temporal fluctuations due to stochastic phenomena like the temperature dependence [17, 18] of the dispersion coefficients, which can become significant in real telecom systems.

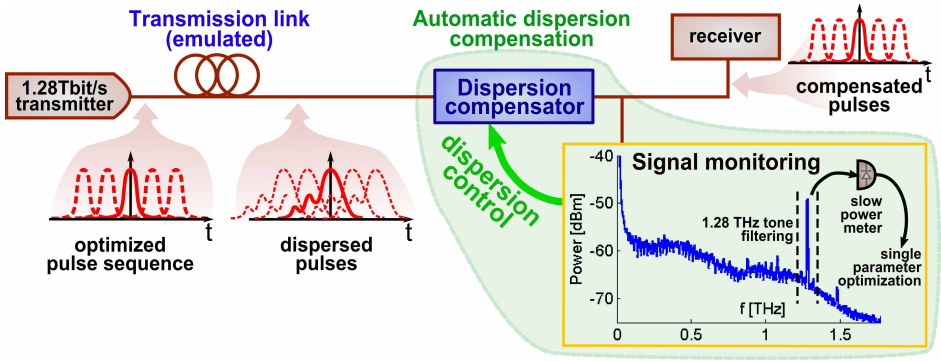

Fig. 1. Automatic dispersion compensation scheme: the 1.28 Tbaud transmitter is followed by a link emulating both initial residual dispersion and dispersion fluctuations. The combination of a signal monitor with a dispersion compensator allows for automatic compensation of those fluctuations simultaneously for β_2, β_3 and β_4. The compensation scheme is based on maximizing the 1.28 THz tone power of the RF spectrum of the signal (right insert).

In this paper we demonstrate automatic and simultaneous compensation of the second, third and fourth orders of dispersion (β_2, β_3 and β_4) for a 1.28 Tb/s single channel OTDM signal. The signal was encoded using on-off keying (OOK) on a pulse train with 275 fs pulsewidth. Our scheme combined all-optical measurement of a single parameter from the RF-spectrum of the signal to monitor the impairments, and spectral pulse-shaping to compensate for disper-

#155613 - $15.00 USD Received 30 Sep 2011; revised 15 Nov 2011; accepted 19 Nov 2011; published 30 Nov 2011

sion [19]. The RF spectrum was measured with a Terahertz bandwidth all-optical RF spectrum analyzer implemented using a chalcogenide photonic chip [20] and, therefore, has the potential for integration to provide a compact solution. Our experiment establishes a key result for transmission of ultra-high baudrate signals.

2. Principles

Various methods have been proposed for monitoring ultra high baud rate signals. Ultra fast optical sampling oscilloscopes provide an averaged pattern of the signal in the time domain [21,22], but present commercial devices do not yet reach Terahertz bandwidth. Optical second harmonic generation (SHG) autocorrelators have been used to access the pulse shape of OOK signals [23], but such devices are bulky and hardly integrable in real communication networks. Other methods based on an all-optical 2R regenerator [24] or a spectral broadening measurement [25] have been proposed.

Here we make use of a chalcogenide photonic-chip-based all-optical RF spectrum analyzer [20, 26] to infer the level of the impairments on the data stream. Techniques based on extracting characteristics of the RF spectrum have already been demonstrated for monitoring multiple impairments on high baud rate systems [7]. In this work the signal quality was monitored using the power of the 1.28 THz tone in the RF spectrum. Feedback control from the monitor to a Spectral Pulse Shaper (SPS) allowed the dispersion state to be adjusted leading to automatic compensation. We evaluated the system on a test bed consisting of a transmission link emulator made of another SPS which was used to apply custom residual dispersion as well as temporal fluctuations. The automatic compensator kept the 1.28 Tbaud signal stable in spite of gradual or even abrupt changes in the link dispersion properties. This scheme is summarized in Fig. 1.

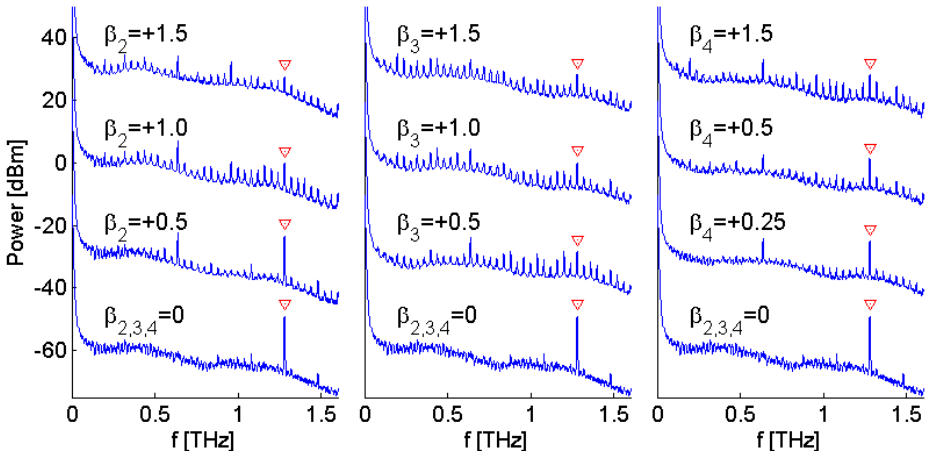

Fig. 2. Evolution of the RF spectrum for the 2^{nd} (left), 3^{rd} (middle) and 4^{th} (right) order of dispersion. For each series of spectra, the bottom graph corresponds to the optimized signal. The application of increasing dispersion reduces the power of the 1.28 THz tone (upper spectra). The dispersion orders β_m are given in the normalized units L_D^m $(m = 2,3,4)$ (see equation 1).

Dispersion compensator: The device used to control the dispersion state of the signal was a Finisar Waveshaper SPS [19]. It allows a custom spectral phase pattern to be applied to an optical field, based on a scheme similar to the one first demonstrated by Weiner et al. [27]. The light spectrum is spread spatially using a conventional grating onto a Liquid Crystal on

#155613 - $15.00 USD Received 30 Sep 2011; revised 15 Nov 2011; accepted 19 Nov 2011; published 30 Nov 2011

Silicon (LCoS) array. The latter allows the phase of light reflected by every pixel to be independently controlled, so that a custom spectral phase can be applied. The modified spectrum is then recombined into the output fiber using the same grating.

GVD corresponds to a quadratic spectral phase, 3^{rd} order dispersion to a cubic spectral phase, and so forth. Any combination of these can be obtained by summing the contributions of each order of dispersion. The dispersion emulation is limited to about $\pm$60ps/nm (for GVD) [19] due to the limited resolution of the SPS, however, this is more than broad enough to allow for residual dispersion compensation in real world applications.

Higher order dispersion monitoring and compensation: Our method extends a previous GVD only compensation scheme [28] by demonstrating that various orders of dispersion can be optimized iteratively by maximizing only the tone power in the RF spectrum. We show that it is not required to extract the explicit values of each order of dispersion. The principle is shown in the right-hand inset of Fig. 1.

The experiment reported below, aims at demonstrating automatic dispersion compensation by cancelling the effect of a dispersion emulator which simulates a transmission link impaired with both residual dispersion and temporal dispersion fluctuations. After propagation through a first SPS, emulating the dispersive link with fluctuations, the signal is sent to a second SPS which performs the compensation. In this proof-of-concept experiment, we emulated GVD and higher-order dispersion fluctuations by applying phase filters corresponding to various combinations of 2^{nd}, 3^{rd} and 4^{th} order dispersion to the first SPS. The second SPS has to react in real time in order to act as a compensator.

Figure 2 shows the RF-spectrum of the data signal measured with an optical spectrum analyzer (OSA) with optimized dispersion, and with 2nd, 3rd and 4th order dispersion. The spectrum of the optimized signal has a maximum 1.28 THz tone power and no peaks at submultiple frequencies (see Fig. 2, bottom spectrum). The addition of a dispersion bias for various orders all impair the RF spectrum by decreasing the fundamental tone power and generating side peaks. (see Fig. 2, other spectra). The values of the dispersion orders β_m in Fig. 2 are given in the normalized units of dispersion length defined by:

$$L_D^m = \frac{1}{\beta_m}\left(\frac{t_{FWHM}}{2\sqrt{ln(2)}}\right)^m \quad \text{where } m \text{ is the order of dispersion.} \tag{1}$$

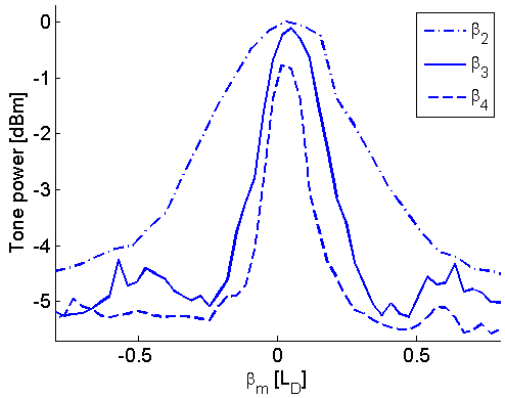

Fig. 3. Impairment on the signal quality (power of the 1.28 THz tone) as a function of three first orders of dispersion. The dispersion orders β_m are given in the normalized units L_D^m $(m = 2,3,4)$ (see equation 1).

#155613 - $15.00 USD Received 30 Sep 2011; revised 15 Nov 2011; accepted 19 Nov 2011; published 30 Nov 2011

We observe that with added dispersion, the power of the 1.28 THz tone reduces and new tones at lower frequencies are always generated. This is caused by broadening of the signal pulses and overlap between subsequent pulses. It is interesting to note that there is no clear qualitative difference between the effects of the various orders of dispersion on the RF spectrum. The key innovation of our approach is that we do not have to distinguish between them. Figure 3 shows the evolution of the tone power independently for the three first orders of dispersion, while all other parameters are fixed to their optimum values.

As dispersion effects are linear, the compensation device can be inserted anywhere between the transmitter and the receiver. In realisitic reconfigurable optical networks, LCoS-based Wavelength Selective Switches (WSS) are already in use at network nodes and could in principle be used to achieve dispersion compensation [19]. Most of previously proposed dispersion compensators would require adding complex optoelectronic components to the backbone of the network.

Compensating the effects of β_2, β_3 and β_4 requires the values of three independent variables to be controlled. The quality factor of the signal (the 1.28 THz tone power) is a single scalar value with a monotonically decreasing dependence on β_2, β_3 and β_4 around the optimum. This allows the existence of a global optimum for the dispersion state, which can be found by running a scalar optimization algorithm on the 3D surface defined by the tone power. A flow diagram of the algorithm is given in Fig. 4.

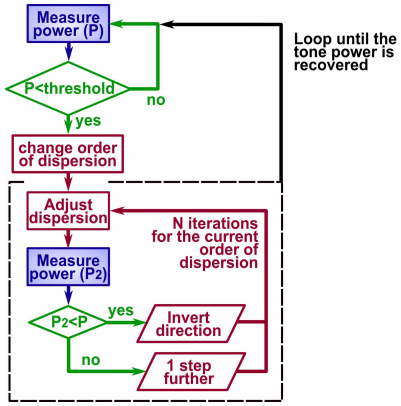

Fig. 4. Flow diagram of the compensation algorithm based on the measurement of the 1.28 THz tone power of the RF spectrum. Once the tone power drops below a threshold due to dispersion impairments, the dispersion compensator changes one order of dispersion in an arbitrary direction. The sign of the change is eventually inverted in case of a further drop in the tone power. The operation is repeated N times (typically $N \approx 4$) for the same order of dispersion. The same process is then applied to another order of dispersion until the tone power has recovered.

3. Experiment

The optical 1.28 Terabaud signal was constructed by time interleaving 32 lower bit rate signals at 40 Gb/s each. In the setup depicted in the upper part of Fig. 5, a pulse train at 40 GHz is delivered by a modelocked optical clock synchronized with an electronic clock signal. The width of the optical pulses, 1.4 ps, is too broad to allow Terabaud time multiplexing without overlap between the channels. Two successive compression stages using highly nonlinear fibers (HNLF) and band-pass filtering (BPF) reduced the length of the pulses to about 275 fs, which were then encoded with a $2^{31} - 1$ pseudo random bit sequence (PRBS) by a Mach-Zehnder modulator

#155613 - $15.00 USD Received 30 Sep 2011; revised 15 Nov 2011; accepted 19 Nov 2011; published 30 Nov 2011

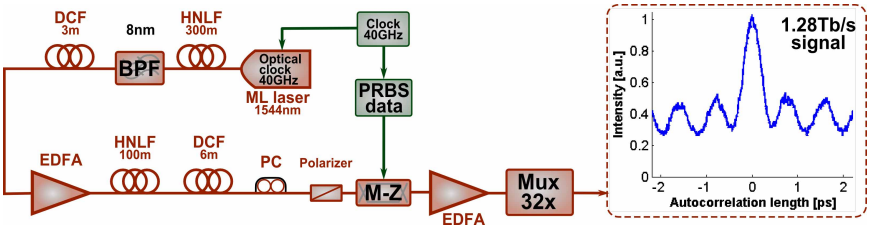

Fig. 5. Generation of the 1.28 Tb/s PRBS signal. A modelocked fiber laser produces a pulse train which is then encoded with a Mach-Zehnder modulator. Two compression stages [29] ensure that the pulses are short enough to avoid overlapping after the time interleaving operation. The autocorrelation trace of the optimized 1.28 Tbaud PRBS signal is measured with a second harmonic generation autocorrelator (right insert).

(M-Z). The 40 Gb/s pulse sequence was then multiplexed to 1.28 Tb/s with 5 interferometric multiplexing stages (Mux). The scheme allowed us to emulate a 1.28 Tb/s signal by replicating 32 times the sequence from a single PRBS generator.

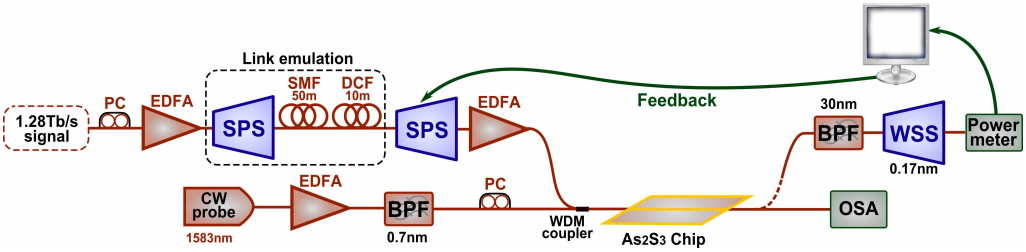

Fig. 6. The dispersion emulation system consists of an SPS and a short fiber link. It is followed by the compensation system controlled by a chip-based all-optical RF spectrum analyzer.

After passing through the dispersion emulation/compensation system, the signal was amplified and combined with a CW probe before propagating through a As_2S_3 dispersion-engineered waveguide [30]. Upon propagation through this highly nonlinear ($\gamma = 10^4$ W^{-1}km^{-1}) waveguide the cw-probe is spectrally broadened by cross-phase modulation (XPM), resulting in an optical spectrum that is proportional to the RF-spectrum of the input signal. We isolate the tone at 1.28 THz with a fiber grating bandpass filter followed with an L-band Wavelength Selective Switch (WSS) configured as an ultra narrow square filter with 0.17 nm bandwidth in order to reject completely the CW component of the probe and the signal and measure the tone power with high contrast using a slow photodiode (PD). The power measured after filtering was typically -55dBm for an optimized signal. Figure 6 depicts the setup used for automatic dispersion compensation, including the RF spectrum analyzer.

4. Results

As multiple orders of dispersion are compensated simultaneously, the cross effects between the various orders has to be taken into account. The actual β_2/β_3 tone power map presents an elliptical peak whose principle axes make an angle with respect to the dispersion coordinates. This makes the global optimum harder to find for the optimization algorithm. We cancelled this effect by applying a linear coordinates transformation consisting of rotating and stretching the reference plane in order to obtain a quasi symmetric peak as shown in Fig. 7. This improves significantly the speed and accuracy of the optimization algorithm. The transformation leads

#155613 - $15.00 USD Received 30 Sep 2011; revised 15 Nov 2011; accepted 19 Nov 2011; published 30 Nov 2011

to the definition of the coordinates $\{\xi_2, \xi_3\}$ in which the algorithm evolves, replacing $\{\beta_2, \beta_3\}$ (the effect is not as strong for β_4, hence does not require such a transformation). Figure 7 shows a color-map of the tone power as a function of ξ_2 and ξ_3 in the units of dispersion lengths (L_{D_2},L_{D_3}). The plot clearly reveals a point of maximum tone power corresponding to the optimized signal (note that the offset with respect to (0,0) is due to the fact that the dispersion compensation of the transmission link was not initially adjusted perfectly).

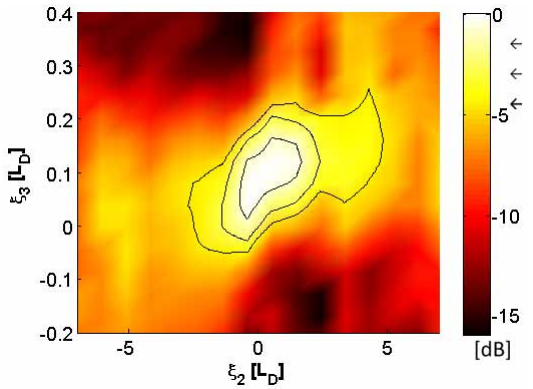

Fig. 7. The colormap shows the tone power as a function of the dispersion state in the modified dispersion coordinates $\{\xi_2, \xi_3\}$ (see text). The three contour plots highlight the optimum zone of the plot at -1.5 dB, -3 dB and -4.5 dB.

Due to the fluctuations of the tone power measured by the powermeter, the algorithm must be robust to noise. Also, during the optimization process it is critical to keep the system operating within a narrow range around the optimum tone power in order to keep the data transmission up at all times. Those requirements prohibit the use of a classical conjugated gradient algorithm due to its instability in noisy configurations. A fixed step steepest gradient method has been run successfully in simulations for compensation of β_2 and β_3. However, the method requires too many evaluations of the tone power for various dispersion states to be applicable when β_4 is added. Therefore, we perform automatic dispersion compensation with a simple fixed step relaxation algorithm, which optimizes the tone power with respect to 2nd, 3rd and 4th order dispersion. The tone power is monitored continuously and once its power drops below a threshold value, the algorithm adjusts the dispersion on the second SPS to recover the optimum tone power. Figure 8 demonstrates the ability of our scheme to accurately track and compensate 2nd, 3rd and 4th order dispersion simultaneously. We emulated a drift of the dispersion by discrete steps via phase profiles applied to the first SPS. It can be seen that our compensation algorithm recovers from the initial drop of the tone power when the dispersion was abruptly changed and after a short time, the tone power returned to its maximum value.

5. Discussion

One can see that the optimum level of the tone power was kept stable over a long period of time. To achieve this we implemented an automatic alignment system for the chalcogenide chip to avoid any slow drift in the coupled power during the experiment. However it should be noted that a drop in the tone power caused by changes to the coupling or due to amplifier failure or any other non dispersive impairment would not necessarily prevent the operation of this automatic dispersion compensator which seeks to relocate a global maximum in tone power. We would also like to note that currently the recovery time when a specific dispersion value is applied to the first SPS is relatively long (typically of the order of 20s for large perturbations), mainly

#155613 - $15.00 USD Received 30 Sep 2011; revised 15 Nov 2011; accepted 19 Nov 2011; published 30 Nov 2011

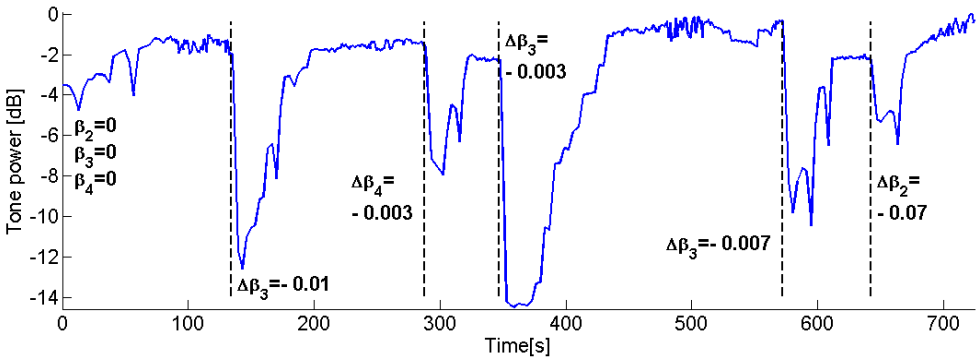

Fig. 8. Automatic dispersion compensation time-line, depicting the temporal evolution of the 1.28 THz tone power of a signal impaired with sharp random dispersion changes. The tone power is quickly recovered thanks to the optimization-algorithm.

due to the use of a relatively slow optimization algorithm, combined with the time required to upload the phase pattern to the SPS and the fetch time from the powermeter. Currently 2nd, 3rd and 4th order dispersion are optimized sequentially, i.e. the algorithm will first try to optimize second-order dispersion for 4 steps and then switch to try to optimize third-order dispersion, and so on. A more efficient algorithm could however greatly reduce this time and recovery times below a second should be feasible. Furthermore, the main origin of dispersion drifts, the temperature dependance of the dispersion coefficient, is an inherently slow effect (of the order of hours or tens of minutes). Therefore, in a deployed system the dispersion drift would be less abrupt, making it much easier for the algorithm to track. Thus our experiments present a worst-case scenario.

6. Conclusion

We have demonstrated automatic tracking and compensation of higher-order dispersion fluctuations of a 1.28 Tb/s signal. This approach greatly facilitates the implementation of high symbol-rate transmission links by eliminating the need for an accurate residual dispersion compensation with specialty fibers and by automatically compensating dispersion drift due to environmental fluctuations.

Acknowledgement

The authors acknowledge the Australian Research Council (ARC) Centres of Excellences Program and an ARC Linkage grant with Finisar Australia. The work of J. Van Erps was supported by the Fund for Scientific Research (FWO Vlaanderen) under a post-doctoral research fellowship, and additionally supported by Belspo-IAP, IWT-SBO, GOA, and the OZR of the Vrije Universiteit Brussel.

#155613 - $15.00 USD Received 30 Sep 2011; revised 15 Nov 2011; accepted 19 Nov 2011; published 30 Nov 2011